ADVANCES IN ATMOSPHERIC SCIENCES, VOL. 30, NO. 4, 2013, 1173–1186

Impact of the North Atlantic Sea Surface Temperature Tripole on the East Asian Summer Monsoon

ZUO Jinqing*[1,2] (左金清), LI Weijing[2] (李维京), SUN Chenghu[2] (孙丞虎), XU Li[3], and REN Hong-Li[2] (任宏利)

[1] *Chinese Academy of Meteorological Sciences, Beijing* 100081

[2] *Laboratory for Climate Studies, National Climate Center, China Meteorological Administration, Beijing* 100081

[3] *Department of Atmospheric, Oceanic and Earth Science, George Mason University, Fairfax, Virginia* 22030*, USA*

(Received 17 June 2012; revised 16 September 2012; accepted 19 October 2012)

ABSTRACT

A strong (weak) East Asian summer monsoon (EASM) is usually concurrent with the tripole pattern of North Atlantic SST anomalies on the interannual timescale during summer, which has positive (negative) SST anomalies in the northwestern North Atlantic and negative (positive) SST anomalies in the subpolar and tropical ocean. The mechanisms responsible for this linkage are diagnosed in the present study. It is shown that a barotropic wave-train pattern occurring over the Atlantic-Eurasia region likely acts as a link between the EASM and the SST tripole during summer. This wave-train pattern is concurrent with geopotential height anomalies over the Ural Mountains, which has a substantial effect on the EASM. Diagnosis based on observations and linear dynamical model results reveals that the mechanism for maintaining the wave-train pattern involves both the anomalous diabatic heating and synoptic eddy-vorticity forcing. Since the North Atlantic SST tripole is closely coupled with the North Atlantic Oscillation (NAO), the relationships between these two factors and the EASM are also examined. It is found that the connection of the EASM with the summer SST tripole is sensitive to the meridional location of the tripole, which is characterized by large seasonal variations due to the north–south movement of the activity centers of the NAO. The SST tripole that has a strong relationship with the EASM appears to be closely coupled with the NAO in the previous spring rather than in the simultaneous summer.

Key words: EASM, North Atlantic SST tripole, diabatic heating, eddy-vorticity forcing, NAO

Citation: Zuo, J. Q., W. J. Li, C. H. Sun, L. Xu, and H.-L. Ren, 2013. Impact of the North Atlantic sea surface temperature tripole on the East Asian summer monsoon. *Adv. Atmos. Sci.*, **30**(4), 1173–1186, doi: 10.1007/s00376-012-2125-5.

1. Introduction

The East Asian summer monsoon (EASM) prevails over China, especially over Eastern China. The summer drought/flood events over this region, which usually cause a large impact on society and the economy, are closely related to EASM variations (Ding, 1992). Owing to the complex nature of the EASM, a better understanding of cause-effect and potential predictors for EASM variability is needed, and thus this issue is a hot topic in the climate research.

EASM variability is influenced by atmospheric circulation anomalies, not only over the tropical and subtropical monsoon region, but also over the middle and high latitudes of the Northern Hemisphere (Zhang and Tao, 1998; Wu and Zhang, 2011). Recent studies have demonstrated that North Atlantic SST anomalies could exert an important impact on East Asian climate variability by inducing a zonal wave-train pattern occurring over the Atlantic-Eurasia region during summer (Wu et al., 2010, 2011). In particular, a strong EASM is usually concurrent with a tripole pattern of SST anomalies in the North Atlantic on the interannual timescale (Wu et al., 2009; Zuo et al., 2012), which features positive SST anomalies in the Northwest Atlantic and negative SST anomalies in the

*Corresponding author: ZUO Jinqing, jqzuo425@126.com

subpolar and tropical ocean, and vice versa. Gu et al (2009) pointed out that this SST tripole also has an important effect on EASM rainfall on the decadal timescale. However, these studies focused mainly on the persistence of the SST tripole from spring through summer, and far too little attention has been paid to the mechanism responsible for the linkage between the tripole and the EASM. Thus, in this study we attempt to answer the question of how the summer SST tripole in the North Atlantic induces changes in atmospheric circulation and then exerts an impact on the EASM on the interannual timescale.

Previous studies have revealed that the North Atlantic Oscillation (NAO), which is believed to be a potential predictor for EASM variability on the interannual timescale (Ogi et al., 2003; Sung et al., 2006), is always followed by the SST tripole in the North Atlantic (Cayan, 1992; Deser and Timlin, 1997; Czaja and Frankignoul, 2002; Zhou et al., 2006). Owing to the strong persistence of the SST tripole from spring through summer, the tripole tends to act as a link between the spring NAO and the EASM (Wu et al., 2009). It has been indicated that the NAO is an atmospheric teleconnection pattern evident in all the seasons of the year in the Northern Hemisphere (Barnston and Livezey, 1987). Nevertheless, the interannual variability of East Asian summer climate is strongly correlated with the NAO and the associated North Atlantic SST tripole in the previous spring rather than in the simultaneous summer (Wu et al., 2009, 2010, 2011). This raises the question as to why the relationship of the EASM with the previous spring NAO is better than that with the simultaneous summer NAO. Thus, another issue to be addressed in this study is whether there are differences in the NAO-induced SST tripole between spring and summer as well as in the relationships between these two factors and the EASM on the interannual timescale.

This paper is composed of six sections. The observational data and two linear dynamic models applied in the study are described in section 2. The linkage between EASM and the North Atlantic summer SST tripole is illustrated in section 3 and the mechanisms responsible for it are explored in section 4. The relationships among the North Atlantic SST tripole, NAO and EASM are further discussed in section 5. Finally, a summary and discussion are given in section 6.

2. Data and models

2.1 *Observational data*

The daily and monthly geopotential height and zonal and meridional wind components, with a horizontal resolution of 2.5°×2.5°, were obtained from the National Centers for Environmental Prediction/National Center for Atmospheric Research (NCEP/NCAR) reanalysis (Kalnay et al., 1996). These variables are available at standard pressure levels and cover the period 1948–2011. This study also employed monthly sensible and latent heat fluxes, as well as 10-m horizontal winds, with 192 equally-spaced longitudinal grid points and 94 unequally-spaced latitudinal grid points, derived from the NCEP/NCAR reanalysis. In addition, we utilized monthly SST data from the National Oceanic and Atmospheric Administration (NOAA) for the period 1948–2011 (Smith et al., 2008). These data have a horizontal resolution of 2.0°×2.0°. The monthly mean rainfall data, with a horizontal resolution of 2.5°×2.5°, were obtained from the Climate Prediction Center (CPC) Merged Analysis of Precipitation (CMAP) (Xie and Arkin, 1997) for the period 1979–2009.

The EASM index used in the study was defined as the difference in regional-averaged 850-hPa zonal wind between the East Asian tropical monsoon trough region (5°–15°N, 90°–130°E) and the East Asian subtropical region (22.5°–32.5°N, 110°–140°E) (Wang and Fan, 1999). A high EASM index denoted a strong EASM, which was generally concurrent with drought in the Yangtze River region in China during summer, and vice versa. According to Li and Wang (2003), the NAO index was calculated based on monthly differences in normalized sea level pressure between 35°N and 65°N over the North Atlantic (80°W–30°E).

To quantitatively describe the interannual variations of the North Atlantic SST tripole that had a strong relationship with the EASM, a SST index (hereinafter referred to as TI) was constructed as the difference between regional-averaged SST anomalies in the middle North Atlantic (34°–44°N, 72°–62°W) and the sum of regional-averaged SST anomalies in the tropics (44°–56°N, 40°–24°W) and in the subpolar ocean (0°–18°N, 46°–24°W). The choice of these domains was based on the linear correlations of the EASM index with SST anomalies in the North Atlantic during summer (Zuo et al., 2012; see their Fig. 3h). During the positive (negative) phase of the SST tripole, SST anomalies were higher (lower) than normal in the Northwest Atlantic, and lower (higher) than normal in the subpolar and tropical ocean. Figure 1 displays the time series of normalized summer TI and EASM indices during the period 1979–2011. It can be seen that the EASM index had a significant in-phase relationship with the summer TI. Their correlation coefficient was 0.55, which was significant at the 95% confidence level.

Owing to the weak correlation between the EASM and the North Atlantic summer SST tripole before

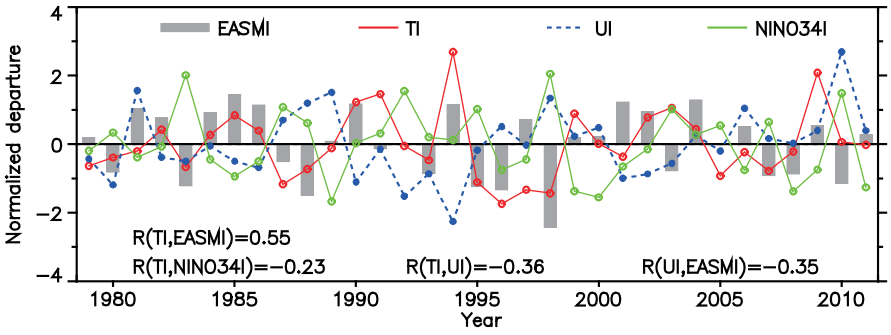

Fig. 1. Time series of the normalized summer tripole SST index (TI), EASM index (EASMI) and Ural geopotential height index (UI), and the preceding winter Nino3.4 SST index (Nino34I) for the period 1979–2011. R is the linear correlation coefficient.

the late 1970s (Zuo et al., 2012), the observational analysis in this study was performed for the period 1979–2011, expect for the moving-correlation shown in Fig. 10. Besides, the linear trends of all the time series were removed before the analysis.

2.2 *Linear dynamic models*

In this study, the role of diabatic heating in maintaining the anomalous low-frequency flow was diagnosed via a linear barotropic model. This model was a time-independent model with a horizontal resolution of T42 and followed a simple barotropic vorticity equation given as:

$$\partial_t \nabla^2 \psi' + J\left(\overline{\psi}, \nabla^2 \psi'\right) + J\left(\psi', \nabla^2 \overline{\psi} + f\right) + \nu \nabla^6 \psi' + \alpha \nabla^2 \psi' = S' \,, \tag{1}$$

where t denotes the time derivative; J represents a Jacobian operator; $\overline{\psi}$ and ψ' are the basic state and perturbation stream functions, respectively; f is the Coriolis parameter; and S' is the anomalous vorticity source induced by the divergent part of the circulation. The barotropic model included a linear damping term that represented the Rayleigh friction, and scale-selective biharmonic diffusion. The biharmonic diffusion coefficient v was selected to dampen the small-scale eddy in one day, while the Rayleigh friction coefficient α was set at $(10\ \mathrm{d})^{-1}$, which ensured that the system was stable at integration (Watanabe, 2004).

The linear baroclinic model employed in this study was a time-dependent model based on primitive equations. The model had a resolution of T42 in the horizontal direction and 20 sigma (σ) levels in the vertical direction. Rayleigh friction and Newtonian damping employed in the model were given as the rate of $(1\ \mathrm{d})^{-1}$ for the lower ($\sigma \leqslant 0.03$) and upper ($\sigma \geqslant 0.9$) levels, and $(30\ \mathrm{d})^{-1}$ for the other levels. The biharmonic diffusion coefficient was $2\times10^{16}\ \mathrm{m}^4\ \mathrm{s}^{-1}$. More details relating to this model can be found in Watanabe and Kimoto (2000) and Watanabe and Jin (2003). With the dissipation terms adopted, the model response took about 20 days to approach a steady state. So, the average of the last five days of a 30-day integration is analyzed in this paper.

3. The linkage between the EASM and the North Atlantic summer SST tripole

To expose the connection between the EASM and the summer SST tripole in the North Atlantic, we employed regression analysis to the summer TI and geopotential height anomalies at 300 hPa, 500 hPa and 850 hPa, respectively. The associated results are given in Fig. 2. Also included in Fig. 2a is the upper-level westerly jet stream represented by the climatological summer mean of 300-hPa zonal wind. It can be seen that a clear zonal wave-train pattern occurs over the Atlantic-Eurasia region. For convenience, this wave-train pattern will be referred to simply as NAE throughout the remainder of the paper. Note that the NAE pattern has the same phase in the lower, middle and upper troposphere, thereby showing an equivalent barotropic structure in the entire troposphere. Associated with the NAE pattern, negative height anomalies prevail over both the subpolar North Atlantic and the region around the Ural Mountains, while positive height anomalies prevail over both the northwest Atlantic and western Europe. These height anomaly centers are mainly located along the upper-level westerly jet stream. The NAE pattern seems to be induced by the North Atlantic summer SST tripole, and the mechanisms that maintain this pattern will be further explored in section 4. In addition, a meridional wave-train pattern can be seen along the East Asian Coast, which is possibly related to the diabatic heating over the tropical Northwest Pacific (Huang and Li, 1987; Nitta, 1987; Huang and Sun, 1992) and thus beyond the scope of this study.

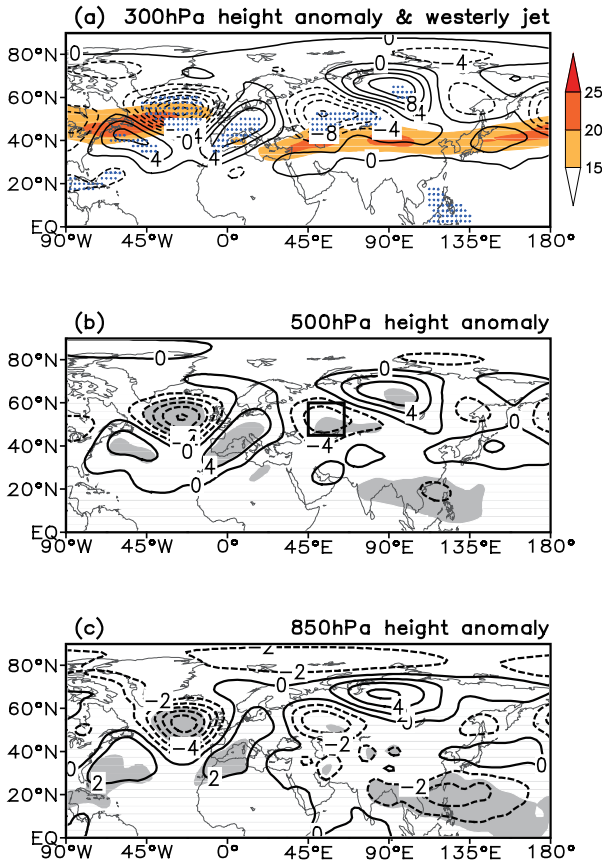

Fig. 2. Geopotential height anomalies (contour; gpm) at (a) 300 hPa, (b) 500 hPa, and (c) 850 hPa, obtained by regressing upon the tripole SST index during summer. Shading in (a) represents the climatological summer mean of 300-hPa zonal wind (m s^{-1}). Dots in (a) and shading in (b) and (c) indicate those regions that are significant at the 95% confidence level. The box in (b) denotes the domain for defining the Ural geopotential height index.

From the above analysis, the EASM and the North Atlantic summer SST tripole appear to be linked by the NAE pattern, which is concurrent with geopotential height anomalies over the region around the Ural Mountains. Many previous studies have revealed that atmospheric circulation anomalies over the Ural Mountains have a substantial effect on the EASM (Zhang and Tao, 1998; Li and Ji, 2001). A positive anomaly of seasonal-mean 500-hPa geopotential height around the Ural Mountains represents intensified blocking activity over this region, which favors an enhanced East Asian subtropical front that tends to result in a weakened EASM, and vice versa. As mentioned above, the negative (positive) geopotential height anomalies over the Ural Mountains coincide with the positive (negative) phase of the North Atlantic SST tripole during summer (Fig. 2), which agrees with the in-phase relationship between the tripole and the EASM (Fig. 1). This result indicates that the impact of the summer SST tripole on the EASM is closely linked to the Ural circulation anomalies. Wu et al. (2009) pointed out that the SST tripole could also result in circulation anomalies over the Okhotsk Sea, but our results show that the regressed geopotential height anomalies over this region are insignificant during summer (Fig. 2).

To support the role of Ural circulation anomalies in linking the EASM and the North Atlantic summer SST tripole, we plotted in Fig. 3 the correlations of summer SST anomalies in the North Atlantic with the summer Ural height index (UI) and EASM index, respectively. The UI here is defined as the regional-averaged 500-hPa geopotential height anomalies in the Ural region (45°–60°N, 45°–65°E). For the convenience of comparison, the sign of the UI has been reversed. It can be seen that the pattern of correlations between the UI and SST anomalies greatly resembles that of the correlations between the EASM index and SST anomalies, not only in shape but also in meridional location, both projecting on the positive tripole mode in the North Atlantic. In addition, the correlation coefficients of the summer UI with the summer TI and EASM index were −0.36 and −0.35, respectively, both of which were significant at the 95% confidence level. These results indicate that geopotential height anomalies around the Ural Mountains have a close relationship with the North Atlantic SST tripole during summer, which supports the conclusion that the former appears to play a key role in linking the SST tripole and the EASM on the interannual timescale.

4. Mechanism diagnostics

The results reported in section 3 suggested that the NAE pattern occurring over the Atlantic-Eurasia region appears to act as a link between the EASM and the North Atlantic summer SST tripole. In this section, the mechanisms responsible for maintaining the NAE pattern are further discussed by focusing on the diabatic heating and synoptic eddy-vorticity forcing, which are the two most important forcings among all forcings to maintain the anomalous low-frequency in middle latitudes (Branstator, 1992; Peng and Whitaker, 1999; Peng et al., 2003).

4.1 *Role of diabatic heating in maintaining the NAE pattern*

The SST anomalies initially induce changes in the local atmospheric circulation through diabatic heating and then could exert an impact on the remote atmospheric circulation by energy dispersion of Rossby

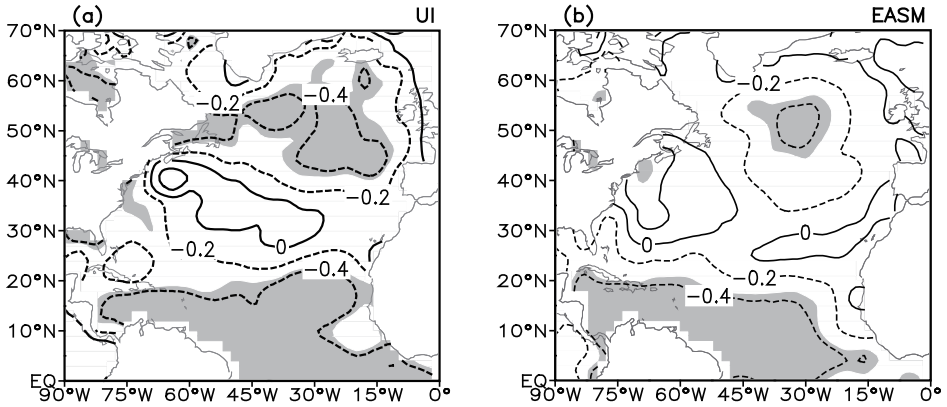

Fig. 3. Correlation coefficients between SST anomalies and (a) Ural geopotential height index (UI) and (b) EASM index during summer. Shading represents those regions that are significant at the 95% confidence level. For convenience of comparison, the sign of UI has been reversed.

waves (Trenberth et al., 1998; Peng and Whitaker, 1999; Peng et al., 2003). Hence, the role of diabatic heating associated with the North Atlantic summer SST tripole in maintaining the NAE pattern is diagnosed.

Figures 4a–c show the anomalies of SST, 500-hPa vertical velocity and precipitation, respectively, obtained by regressing upon the TI during summer. Positive (negative) values of vertical velocity denote rising (sinking) motion. Owing to the similar pattern of regressed anomalies between the positive and negative phases of the SST tripole, except for a reversal in the sign, a detailed description is only given for the positive phase as follows. It is shown that there are positive SST anomalies in the Northwest Atlantic between 30°N and 45°N, and negative SST anomalies in the tropical North Atlantic between 5°N and 15°N, as well as in the subpolar ocean between 45°N and 60°N (Fig. 4a). Anomalous descent at 500 hPa (Fig. 4b) and below-normal precipitation (Fig. 4c) are seen over the tropical North Atlantic where the SST anomalies are negative, thereby indicating a suppressed convective activity by the cold SST anomaly. To balance the anomalous descent in the troposphere, anomalous convergent flow prevails in the upper troposphere (data not shown), which further triggers an anomalous Rossby wave source (Sardeshmuhk and Hoskins, 1988) and thus tends to provide a forcing for maintaining the NAE pattern. Negative precipitation anomalies can be seen over the middle North Atlantic, which are concurrent with the positive local SST anomalies, indicating that the associated diabatic heating appears to be insignificant over this region.

As expected, anomalous cyclonic flow prevails in the upper troposphere (Fig. 2a) and anticyclonic flow in the lower troposphere (Fig. 2c) over the Caribbean Sea and the adjacent regions, which feature a Gill-type response (Gill, 1980) to the tropical North Atlantic cooling. Note that a meridional wave-train pattern of geopotential height anomalies can be seen along the North American East Coast (Fig. 2), which is connected with the NAE pattern. These results indicate that the maintenance of the NAE pattern appears to depend on the tropical North Atlantic diabatic heating.

To confirm the role of diabatic heating in maintaining the NAE pattern, in Fig. 4d we show the turbulent heat flux (the sum of sensible and latent heat flux, and hereinafter referred to as SHLE) anomalies obtained by regressing upon the TI during summer. Positive (negative) SHLE indicates heat flux out of (into) the ocean surface. The 10-m horizontal wind anomalies regressed upon the TI is also included in Fig. 4d. Negative SHLE anomalies can be seen over the Northeast Atlantic between 10°N and 30°N, which are concurrent with the negative SST anomalies and neutral surface wind anomalies over this region. This indicates that the SST plays an active role in determining SHLE anomalies in the low latitudes of the North Atlantic. On the other hand, weak and positive SHLE anomalies are found over the western subtropical North Atlantic, corresponding to the warm SST anomalies, but less precipitation and southerly anomalies are found over this region. Moreover, positive SHLE anomalies can be seen over the subpolar North Atlantic, which are concurrent with the cold SST anomalies and strengthened westerlies over this region. Therefore, it appears that the positive SHLE anomalies over the subtropical (subpolar) North Atlantic mainly result from the strengthened southerly (westerly) flows, suggesting that atmospheric circulation plays a dominant role in determining the SHLE and SST anomalies in the extratropical

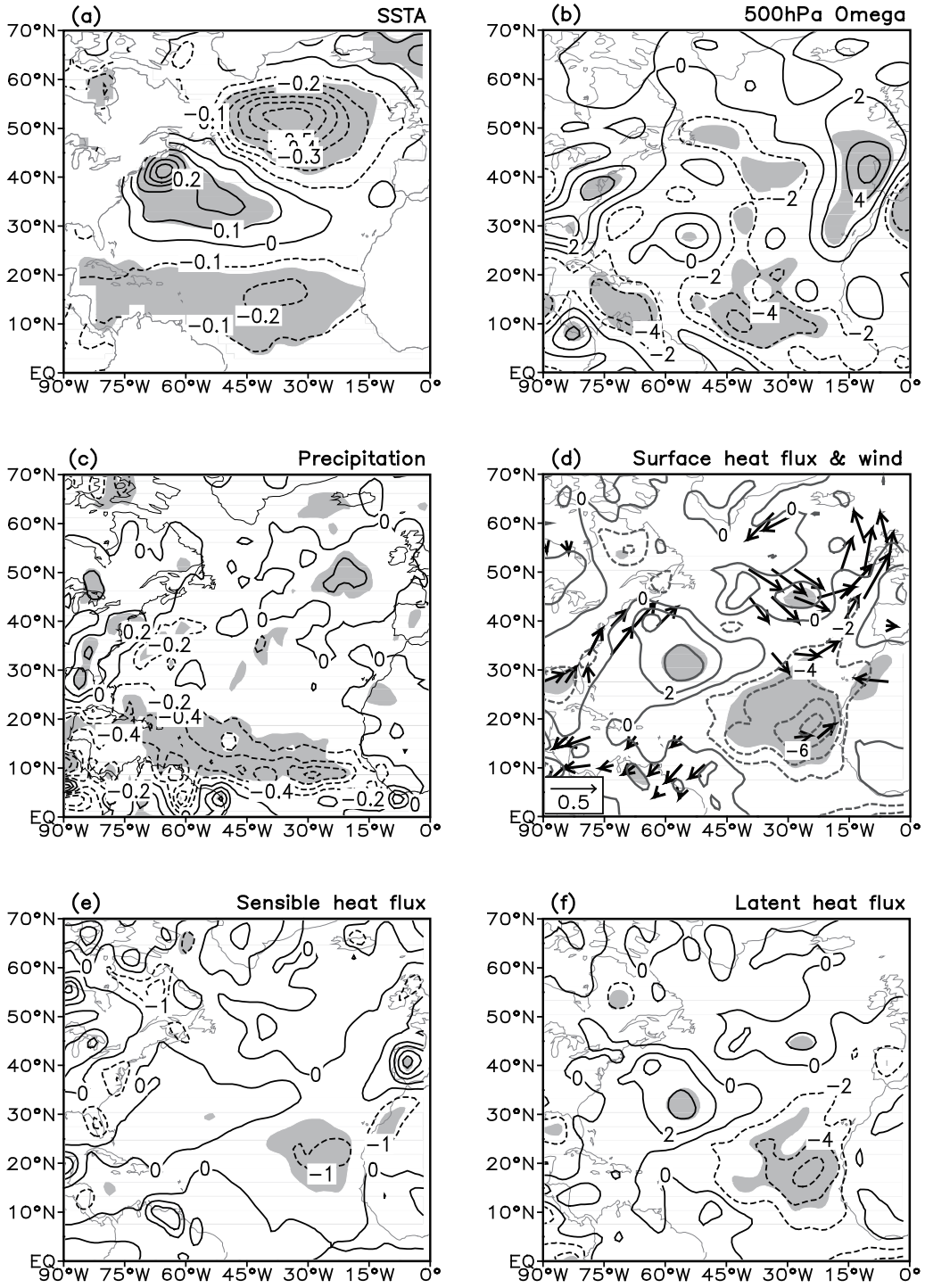

Fig. 4. (a) SST anomalies (K) obtained by regressing upon the tripole SST index during summer. Shading represents those regions that are significant at the 95% confidence level. (b) The same as in (a), but for the vertical velocity anomaly (10^{-3} Pa s^{-1}) at 500 hPa. Positive values in (b) denote rising motion. (c) The same as in (a), but for the precipitation anomaly (mm d^{-1}). (d) The same as in (a), but for the anomalies of total heat flux (sum of latent and sensible heat flux; contour; W m^{-2}) and 10-m horizontal wind vectors (vector; m s^{-1}). (e–f) The same as in (a), but for sensible and latent heat flux anomalies (W m^{-2}), respectively. A positive (negative) heat flux anomaly indicates heat flux out of (into) the ocean surface.

North Atlantic. To examine the respective contribution of sensible heat flux (SH) and latent heat flux (LE) to the SHLE, regression analysis was further applied to the summer TI and SH and LE anomalies, respectively. The results show that the SH anomalies are relatively weak over almost the whole North Atlantic (Fig. 4e), but the pattern of the LE anomalies (Fig. 4f) resembles closely that of the SHLE anomalies in the North Atlantic (Fig. 4d). Moreover, the magnitude of LE anomalies is comparable with that of SHLE anomalies. Therefore, the SHLE anomalies associated with the North Atlantic SST tripole are mainly determined by the LE anomalies during summer. These results support the importance of the role of tropical North Atlantic diabatic heating in maintaining the NAE pattern.

Further evidence for the connection of the NAE pattern with tropical North Atlantic diabatic heating is given in Fig. 5a, which shows the 500-hPa stream function anomaly and associated wave-activity flux (WAF) (Takaya and Nakamura, 2001) obtained by regressing upon the TI during summer. Associated with the NAE pattern, there are significant WAFs extended

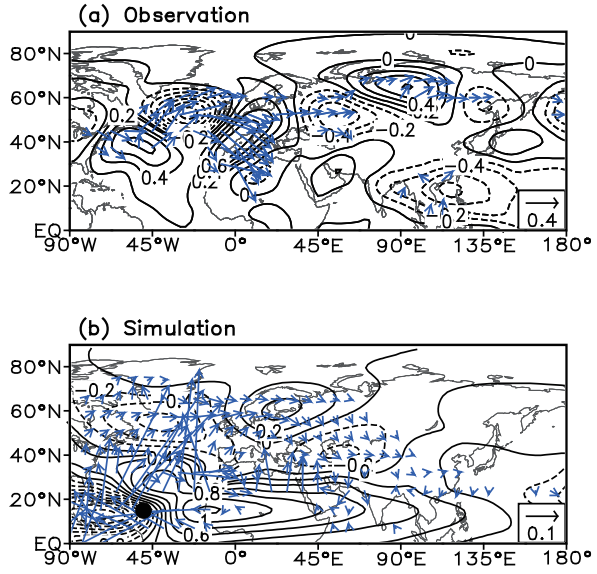

Fig. 5. (a) 500-hPa stream function anomaly (contour; 10^6 m^2 s^{-1}) and the associated wave-activity flux (vector; m^2 s^{-2}) obtained by regressing upon the tripole SST index during summer. (b) The same as in (a), but for the steady barotropic model response to the idealized vorticity forcing centered at (15°N, 50°W) (denoted by a closed circle).

northward from the middle North Atlantic to the subpolar ocean and then divided into two branches. One is southward to North Africa, and the other eastward to the region around the Ural Mountains. This suggests that tropical North Atlantic diabatic heating makes an important contribution to Atlantic–Eurasian circulation change through the NAE pattern.

Owing to the barotropic nature of the NAE pattern and its possible connection with tropical North Atlantic diabatic heating, processes that generate the height anomalies are conceivably understood in a barotropic vorticity equation (Branstator, 1983). For this purpose, an idealized experiment was conducted by using the linear barotropic model forced by the anomalous vorticity source. Based on the 500-hPa vertical velocity and precipitation anomalies shown in Figs. 4b and c, the prescribed vorticity forcing in the model was placed over the tropical North Atlantic with a maximum of 2.0×10^{-11} s^{-2} at (15°N, 50°W). The model was linearized about the climatological summer mean of the 300-hPa stream function derived from the NCEP/NCAR reanalysis. Figure 5b shows the stream function response and associated WAF to the idealized vorticity forcing. A clear wave-train pattern was found over the Atlantic-Eurasia region (Fig. 5b), which resembles the observed NAE pattern (Fig. 5a). In particular, anomalous cyclonic flows were identified over the Ural Mountains in both the model and observations, though the former shifted southward compared with the latter. These results support the importance of the role of tropical North Atlantic diabatic heating in maintaining the NAE pattern. Note that the stream function response in the model was smaller compared with the observational regression over the middle North Atlantic, but larger over the tropics. Actually, the observational regression reflected the equilibrium state among all the forcings. This implies that other factors, such as transient eddy forcing, may make an important contribution to maintaining the NAE pattern.

4.2 *Role of synoptic eddy-vorticity forcing in enhancing the NAE pattern*

In addition to diabatic heating, synoptic eddy forcing is another of the most important forcings in maintaining the anomalous low-frequency flow over the middle latitudes (Lau and Nath, 1991; Kug and Jin, 2009; Ren et al., 2009). In particular, synoptic eddy-vorticity forcing is the most important component of the eddy forcings (Branstator, 1992). Previous numerical studies have revealed that synoptic eddy-vorticity forcing is of vital importance to maintaining the atmospheric response to the North Atlantic SST anomalies during winter (Watanabe and Kimoto, 2000; Peng et al., 2003; Li, 2004; Li et al., 2007; Pan, 2007; Han et al, 2011). However, synoptic eddy forcing is sensitive to the background flow (Peng and Whitaker, 1999).

Hence, the role of synoptic eddy-vorticity forcing associated with the North Atlantic summer SST tripole in maintaining the NAE pattern is investigated.

According to the quasi-geostrophic potential vorticity equation, the synoptic eddy-vorticity feedback to the anomalous low-frequency flow could be depicted by a stream function tendency (ψ_t) satisfying the relationship as (Lau and Holopainen, 1984):

$$\nabla^2 \psi_t = -\nabla \cdot \overline{\boldsymbol{V}'\zeta'} \,, \tag{2}$$

where $\boldsymbol{V}$ and ζ are the horizontal wind vector and relative vorticity, respectively. Here, the prime represents the synoptic-eddy component, and the overbar denotes a time average. To obtain the synoptic-eddy component, we applied the Lanczos filter (Duchon, 1979) to the daily zonal and meridional winds for the period ranging from two to eight days. The stream function tendency due to synoptic eddy-vorticity forcing was obtained by solving the Poisson equation.

Since synoptic eddy-vorticity forcing is highly correlated with storm-track activity, we examine both the anomalies of storm-track activity (Fig. 6a) and the eddy-induced stream function tendency at 300 hPa (Fig. 6b) obtained by regressing upon the TI during summer. The storm-track activity is represented by the root mean square of band-pass filtered (2–8 days) 500-hPa geopotential height. Also included in Figs. 6a and b are the climatological summer mean of storm-track activity and 300-hPa zonal wind, respectively. Owing to the barotropic nature of synoptic eddy-vorticity forcing and its largest effect on the low-frequency flow in the upper troposphere (Lau and Nath, 1991; Branstator, 1992), regression analysis was only applied to the 300-hPa eddy-induced stream function tendency in this study. We find that the regressed anomalies of storm-track activity show a north–south dipole straddling its mean position over the North Atlantic (Fig. 6a). During the positive phase of the North Atlantic SST tripole, the storm-track activity is enhanced on the south side and weakened in the north, which indicates a southward shift of the storm-track activity. Moreover, obvious and negative eddy-induced stream function tendency can be seen over the region near the North Atlantic upper-level westerly jet exit (Fig. 6b), which coincides with the negative geopotential height anomaly over this region (Fig. 2), thereby indicating a positive eddy-vorticity feedback. The negative eddy-induced stream function tendency also coincides with the southward shift of the storm-track activity over the North Atlantic, which indicates that the synoptic eddy-vorticity forcing is closely related to changes in the storm-track activity. An opposite sce-

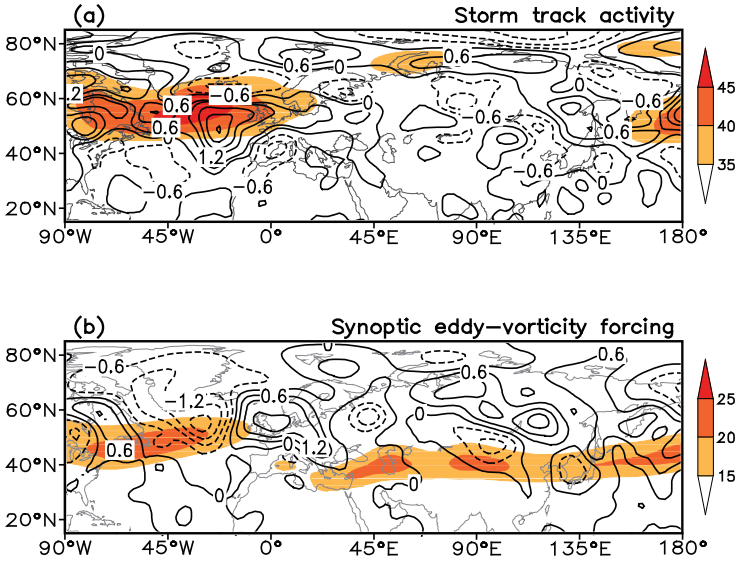

Fig. 6. (a) Anomalies of the storm-track activity (contour) obtained by regressing upon the tripole SST index during summer. The storm-track activity is defined as the root mean square of band-pass filtered 500-hPa geopotential height in the period of 2–8 days. Shading indicates the climatological summer mean of storm-track activity. Units are gpm. (b) The same as in (a), but for the stream function tendency (contour; $m^2\ s^{-2}$) due to synoptic eddy-vorticity forcing at 300 hPa. Shading represents the climatological summer mean of zonal wind for the same layer ($m\ s^{-1}$).

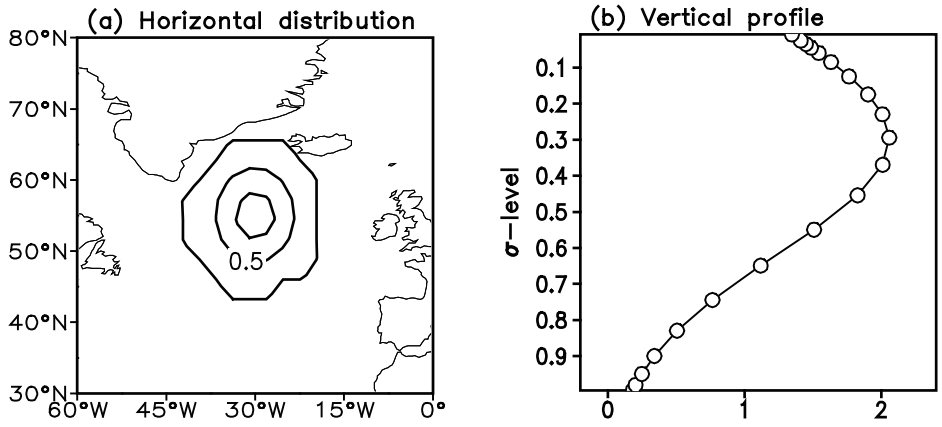

Fig. 7. (a) The vertical mean of eddy-vorticity forcing and (b) vertical profile of the forcing centered at (55°N, 30°W). Units: 10^{-11} s^{-2}.

nario can be seen for the negative phase of the North Atlantic SST tripole. There, results suggest that the synoptic eddy-vorticity flux divergence associated with the North Atlantic SST tripole appears to play an important role in maintaining the NAE pattern via a positive feedback mechanism during summer.

Linear baroclinic models are useful tools to diagnose the mechanism for maintaining the anomalous low-frequency flow by synoptic eddy forcing (Watanabe and Kimoto, 2000; Peng et al., 2003). Thus, an idealized experiment was performed by using a linear baroclinic model to confirm the role of synoptic eddy-vorticity forcing in maintaining the NAE pattern. For this experiment, the model was linearized about the summer climatology derived from the NCEP/NCAR reanalysis and forced by the synoptic eddy-vorticity flux divergence, which acted as the synoptic eddy-vorticity forcing. The horizontal distribution of depth-averaged eddy-vorticity forcing and the vertical profile of the maximum forcing in the initial state are given in Fig. 7. According to the observed eddy-induced stream function tendency (Fig. 6b), the eddy-vorticity forcing in the model was centered at σ=0.29 in the vertical direction and (55°N, 30°W) in the horizontal direction. As shown in Fig. 8, these idealized eddy-vorticity forcings applied to the baroclinic model triggered a negative stream function response right over the region where the forcings were placed, and two branches of Rossby waves to the east. One was southeastward to North Africa, and the other was eastward to East Asia, which resulted in a negative stream function response over the Ural Mountains. Note that the pattern of stream function response in the baroclinic model greatly resembled the observations shown in Fig. 5a. Therefore, the consistency between model simulation and observations is strong enough to support an active role of synoptic eddy-vorticity forcing in enhancing the NAE pattern during summer.

Experiments with an atmospheric general circulation model and a diagnostic linear baroclinic model by Li et al. (2007) suggested that the extratropical response to a tropical Atlantic SST anomaly is maintained primarily by synoptic eddy-vorticity forcing during winter. In other words, synoptic eddy-vorticity

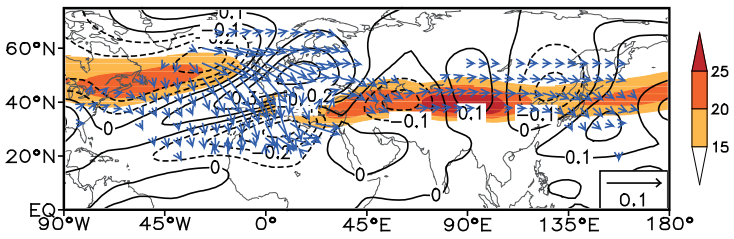

Fig. 8. Steady baroclinic model response as represented by the stream function (contour; 10^6 m^2 s^{-1}) and the associated wave-activity flux (vector; m^2 s^{-2}) at σ=0.29 to the idealized eddy-vorticity forcing shown in Fig. 7. Shading denotes the climatological summer mean of zonal wind (m s^{-1}) for the same layer.

forcing is of vital importance in maintaining the atmospheric response to the North Atlantic SST anomalies during both winter and summer.

Also of note is that the Asian response (Fig. 8) is mainly trapped in the upper-level westerly jet, whereas the observed anomalies in the NAE pattern (Fig. 2a) prevail along the poleward flank of the Asian jet. Namely, the position of the NAE pattern in Fig. 8 relative to the upper-level jet is different from that seen in observations over Asia. It has been demonstrated that two-way synoptic eddy and low-frequency (SELF) feedback plays an essential role in generating the low-frequency anomalies in the extratropics (Jin et al., 2006; Pan et al., 2006; Ren et al., 2012), but synoptic eddy forcing is just considered as an external forcing in the linear model used in this study. Therefore, a lack of two-way SELF feedback may contribute to the aforementioned difference between the model simulation and observations.

5. Relationships among the North Atlantic SST tripole, NAO and EASM

The tripole-like SST anomalies in the North Atlantic Ocean primarily result from the NAO-like dipole in the atmospheric circulation (Cayan, 1992; Deser and Timlin, 1997; Czaja and Frankignoul, 2002; Zhou et al., 2006). Given this, is the North Atlantic summer SST tripole that has a strong relationship with the EASM (referred to as the EASM-related SST tripole) coupled with the simultaneous summer NAO? To address this question, we calculated the correlation coefficients between SST anomalies in the North Atlantic and the NAO index during summer, and the results are shown in Fig. 9a. It can be seen that the correlations show a clear tripole pattern in the North Atlantic, which suggests that the SST tripole is closely coupled with the NAO during summer. A comparison of Fig. 9a and Fig. 3b reveals that the summer NAO-coupled SST tripole resembles closely the EASM-related SST tripole in shape, but the location of the former is about 5°–10° northward compared with that of the latter. The summer NAO-coupled SST tripole is mainly located in the extratropics northward of about 20°N, while the EASM-related SST tripole has significant SST anomalies in the tropics southward of about 20°N. These results imply the EASM-related SST tripole seems to have no significant relationship with the simultaneous summer NAO.

It has been indicated that the activity centers of the NAO would move northward systematically from winter to summer (Barnston and Livezey, 1987), which may lead to seasonal changes in the meridional location of the NAO-induced SST tripole in the North Atlantic. This raises the possibility that the EASM-related SST tripole may be linked to the previous spring NAO. Thus, in Fig. 9b we display the correlations between SST anomalies in the North Atlantic and the NAO index during spring. It can be seen that their correlations exhibit a tripole pattern in the North Atlantic, thereby indicating that the SST tripole is also coupled with the NAO during spring. Moreover, the NAO-coupled SST tripole in the spring is located more southward than that in the summer. The former resembles closely the EASM-related SST tripole not only in shape but also in meridional location. These results indicate that the summer SST tripole that has a strong relationship with the EASM tends to result from the NAO in the previous spring rather than in the simultaneous summer.

To further understand the relationships among the EASM, North Atlantic SST tripole and NAO on the

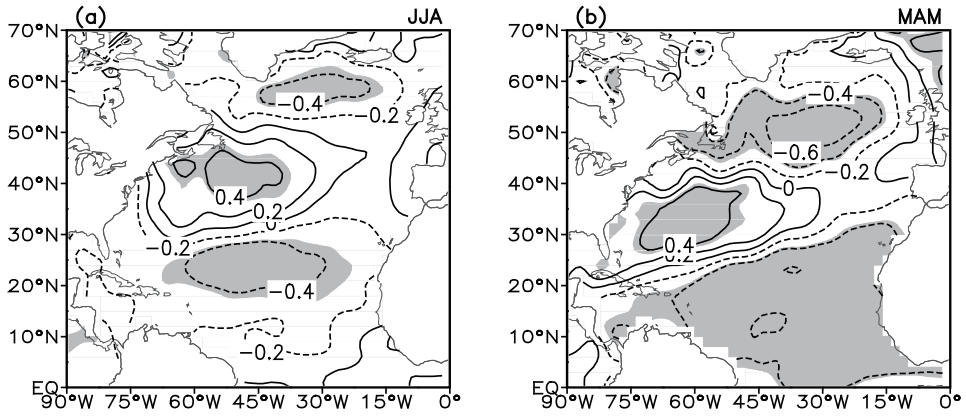

Fig. 9. Correlation coefficients between the NAO index and SST anomalies during (a) summer and (b) spring. Shading represents those regions that are significant at the 95% confidence level.

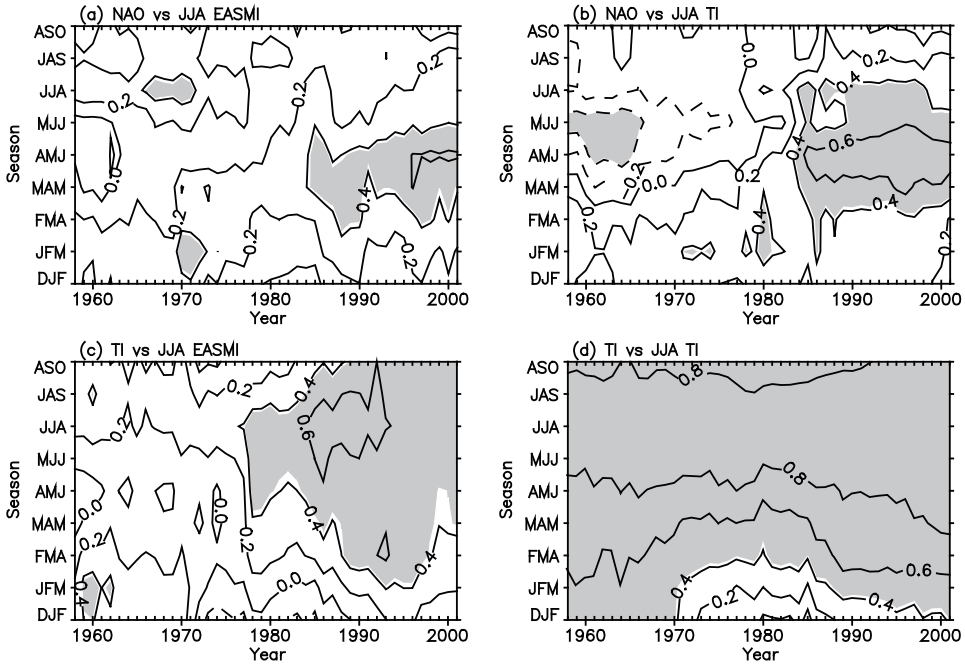

Fig. 10. Lead/lag moving-correlations between summer EASM index (EASMI) and 3-month-running-averaged NAO indices from the preceding January to the following September with a 21-yr moving window for the period 1948–2011. Shading shows significance at the 95% confidence level. (b) The same as in (a), but for the summer tripole SST index (TI). (c) The same as in (a), but for the summer EASMI and the 3-month-running-averaged TI from the preceding January to the following September. (d) The same as in (c), but for the summer TI.

interannual timescale, in Fig. 10a (Fig. 10b) we show the lead/lag moving-correlations between the summer EASM index (TI) and the 3-month-running-avaraged NAO indices from the preceding January to the following September with a 21-yr moving window for the period 1948–2011. We also calculated the lead/lag moving-correlations between the EASM index and 3-month-running-avaraged TI for the same period, as shown in Fig. 10c. Note that the TI here is to describe the interannual variations of the EASM-related SST tripole. It can be seen that the summer EASM index and TI are both correlated most closely with the previous spring NAO index, while the EASM index is linked most closely to the simultaneous summer TI, though their sliding correlations are all characterized by large decadal variations. The decadal changes in the relationships among the EASM, TI and NAO indices occur in the late 1970s, a possible mechanism for which was given in our previous study (Zuo et al., 2012). These results support the conclusion that the summer SST tripole that has a significant impact on the EASM is closely related to the NAO in the previous spring rather than in the simultaneous summer.

To briefly investigate the persistence of the North Atlantic SST tripole, the lead/lag sliding cross-autocorrelations of the summer TI were calculated (see Fig. 10d). We can see that the summer TI is correlated closely with the previous spring TI for the whole period from 1948 to 2011, which indicates the SST tripole has a relatively strong persistence from spring through summer, being in good agreement with previous work (Wu et al., 2009). The seasonal northward movement of the activity centers of the NAO tends to provide favorable conditions for the NAO-induced SST tripole to persist from spring through summer.

We can infer from the above results that the impact of the North Atlantic summer SST tripole on the EASM is sensitive to the meridional location of the tripole. In order to confirm this hypothesis, another idealized experiment was performed by using the linear barotropic model. In this experiment, the horizontal distribution of the anomalous vorticity forcing was the same as in Fig. 5b, except the center for maximum forcing shifted 10° northward and was located at (25°N, 50°W). The steady stream function response and the associated WAF to this idealized vorticity forcing are given in Fig. 11. Note that a clear wave-train pattern propagated from the subtropical North Atlantic to Western Europe, and then divided into two branches. One was northeastward to Eurasia north-

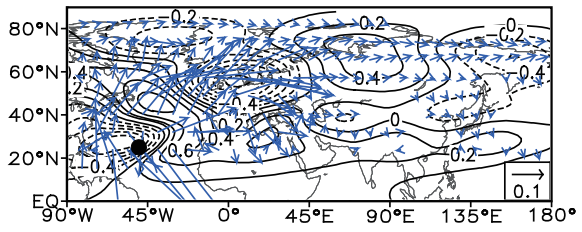

Fig. 11. The same as in Fig. 5b, but for the idealized vorticity forcing with a maximum centered at (25°N, 50°W).

ward of about 60°N, and the other southward to North Africa. There was no obvious stream function response over the Ural Mountains and East Asia. By comparing Fig. 11 with Fig. 5b, we can see that there was a significant difference in the pathways of the atmospheric wave-train response to the idealized vorticity forcing with different meridional location, supporting the hypothesis that the impact of the summer SST tripole on the EASM is sensitive to the meridional location of the tripole. Our conclusion is also supported by previous studies in which it was demonstrated that the pattern of the atmospheric response to the heating with different meridional locations may be different because the synoptic eddy-vorticity feedback depends on the position of the heating relative to the storm track (Peng and Whitaker, 1999; Li et al., 2006).

6. Summary and discussion

A strong (weak) EASM is usually concurrent with the North Atlantic summer SST tripole on the interannual timescale, which has positive (negative) SST anomalies in the Northwest Atlantic and negative (positive) SST anomalies in the subpolar and tropical ocean. In the present study, the mechanism responsible for this linkage was diagnosed by using observations for the period 1979–2011. It has been shown that the NAE pattern occurring over the Atlantic-Eurasia region appears to act as a link between the EASM and the summer SST tripole. The NAE pattern is concurrent with the geopotential height anomaly over the region around the Ural Mountains, which has a substantial effect on the EASM. Further diagnosis based on observations and a linear barotropic model revealed that the maintenance of the NAE pattern appears to depend on the diabatic heating associated with the tropical North Atlantic SST anomaly. On the other hand, the NAE pattern in turn induces a southward/northward shift of the storm-track activity over the North Atlantic, which tends to result in a positive eddy-vorticity feedback, and thus enhances the NAE pattern. Diagnosis based on a linear baroclinic model confirmed the active role of synoptic eddy-vorticity forcing in maintaining the NAE pattern.

Since the North Atlantic SST tripole mainly results from the driving of the NAO-like atmospheric forcing, relationships between these two factors and the EASM were further investigated on the interannual timescale. It was revealed that the summer SST tripole that has a strong relationship with the EASM is closely coupled with the NAO in the preceding spring rather than in the simultaneous summer, which appears to be attributable to the seasonal north–south movement of the activity centers of the NAO. The spring NAO-coupled SST tripole has pronounced SST anomalies in the tropics, while the summer NAO-coupled SST tripole is mainly confined to the extratropics due to the northward shift of the summer NAO itself. Barotropic modeling results confirmed that the type of SST tripole located in the extratropics has no significant impact on the EASM. Therefore, the relationship of the EASM with the North Atlantic summer SST tripole is sensitive to the meridional location of the tripole on the interannual timescale.

The present analysis indicates that the tropical component of the North Atlantic summer SST tripole plays the key role in influencing the EASM. On the other hand, SST changes in the tropical North Atlantic are influenced strongly not only by the NAO, but also by ENSO [Xie and Carton (2004), and references therein]. Thus, a question arises as to whether the results regarding the linkage between the North Atlantic summer SST tripole and EASM are contaminated by the ENSO signals. As illustrated by Wu et al. (2011), the relationship between the North Atlantic spring SST tripole and the preceding winter ENSO is significant in the 1980s and 1990s, but weak in the latest decade. In this study, we found that the correlation coefficient between the summer tripole SST index and the preceding winter Nino3.4 SST was only −0.23 for the period 1979–2011 (Fig. 1), which is not significant at the 90% confidence level. In addition, the NAE pattern that acts as a link between the North Atlantic summer SST tripole and EASM was still robust after removing the ENSO signals from the summer tripole SST index and the atmospheric fields based on a linear regression method using the winter-mean Nino3.4 SST index (data not shown). Therefore, it appears that the relationship between the North Atlantic summer SST tripole and EASM is independent of ENSO during the period analyzed in this study. Wu et al. (2011) suggested that the North Atlantic SST tripole can have an impact on Northeast China summer temperature, independent of ENSO, which is in agreement with our conclusions.

Previous numerical studies have suggested that

SST anomalies in the extratropical North Atlantic tend to have a considerable impact on atmospheric circulation (Peng et al., 2003; Li, 2004). This raises the possibility that extratropical SST anomalies corresponding to the North Atlantic summer SST tripole may make a contribution to the linkage between the tripole and the EASM, which is, however, hard to identify by observational diagnosis due to the dominant role of the atmosphere during the interannual ocean–atmosphere interaction processes over this region. Though the numerical simulation by Watanabe and Kimoto (2000) revealed that the mid-latitude SST anomaly corresponding to the North Atlantic SST tripole has positive feedback on the anomalous atmospheric circulation during winter, observational analysis in this study indicated that its effect appears to be relatively weak during summer. However, more studies are needed to identify the relative contribution of the tropical and extratropical SST anomalies corresponding to the North Atlantic summer SST tripole by using climate models in which the atmospheric intrinsic variability could be well reproduced.

Acknowledgements. The authors are grateful for the linear dynamic models provided by Dr. M. WATANABE and the useful comments and suggestions of the two anonymous reviewers. We also thank Dr. WU Bingyi for carefully reading an early draft of this article and offering constructive criticism. This work was jointly supported by the National Basic Research Program of China (Grant Nos. 2010CB950404, 2013CB430203, 2010CB950501 and 2012CB955901), the National Natural Science Foundation of China (Grant No. 41205058), the China Postdoctoral Science Foundation (Grant No. 2012M510634), and the National Science and Technology Support Program of China (Grant No. 2009BAC51B05).

REFERENCES

Barnston, A. G., and R. E. Livezey, 1987: Classification, seasonality and persistence of low-frequency atmospheric circulation patterns. *Mon. Wea. Rev.*, **115**, 1083–1126.

Branstator, G., 1983: Horizontal energy propagation in a barotropic atmosphere with meridional and zonal structure. *J. Atmos. Sci.*, **40**, 1689–1708.

Branstator, G., 1992: The maintenance of low-frequency atmospheric anomalies. *J. Atmos. Sci.*, **49**, 1924–1945.

Cayan, D. R., 1992: Latent and sensible heat flux anomalies over the northern oceans: Driving the sea surface temperature. *J. Phys. Oceanogr.*, **22**, 859–881.

Czaja, A., and C. Frankignoul, 2002: Observed impact of Atlantic SST anomalies on the North Atlantic oscillation. *J. Climate*, **15**, 606–623.

Deser, C., and M. Timlin, 1997: Atmosphere-ocean interaction on weekly timescales in the North Atlantic and Pacific. *J. Climate*, **10**, 393–408.

Ding, Y. H., 1992: Summer monsoon rainfalls in China. *J. Meteor. Soc. Japan.*, **70**, 373–396.

Duchon, C., 1979: Lanczos filtering in one and two dimensions. *J. Appl. Meteor.*, **18**, 1016–1022.

Gill, A. E., 1980: Some simple solutions for heat-induced tropical circulation. *Quart. J. Roy. Meteor. Soc.*, **106**, 447–462.

Gu, W., C. Y. Li, X. Wang, W. Zhou, and W. J. Li, 2009: Linkage between mei-yu precipitation and North Atlantic SST on the decadal timescale. *Adv. Atmos. Sci.*, **26**, 101–108, doi: 10.1007/s00376-009-0101-5.

Han, Z., S. Li, and M. Mu, 2011: The role of warm North Atlantic SST in the formation of positive height anomalies over the Ural Mountains during January 2008. *Adv. Atmos. Sci.*, **28**, 246–256, doi: 10.1007/s00376-010-0069-1.

Huang, R. H., and W. J. Li, 1987: Influence of the anomaly of heat source over the northwestern tropical Pacific for the subtropical high over East Asia. *Proc. Inter. Conf. on the General Circulation of East Asia*, Chengdu, China, 40–45.

Huang, R. H., and F. Y. Sun, 1992: Impacts of the tropical western Pacific on the East Asian summer monsoon. *J. Meteor. Soc. Japan.*, **70**, 243–256.

Jin, F.-F., L.-L. Pan, and M. Watanabe, 2006: Dynamics of synoptic eddy and low-frequency flow interaction. Part I: A linear closure. *J. Atmos. Sci.*, **63**, 1677–1694.

Kalnay, E., and Coauthors, 1996: The NCEP/NCAR 40–year reanalysis project. *Bull. Amer. Meteor. Soc.*, **77**, 437–472.

Kug, J.-S., and F.-F. Jin, 2009: Left-hand rule for synoptic eddy feedback on low-frequency flow. *Geophys. Res. Lett.*, **36**, L05709, doi: 10.1029/2008GL036435.

Lau, N.-C., and E. O. Holopainen, 1984: Transient eddy forcing of the time-mean flow as indentified by geopotential tendencies. *J. Atmos. Sci.*, **41**, 313–328.

Lau, N.-C., and M. J. Nath, 1991: Variability of the baroclinic and barotropic transient eddy forcing associated with monthly changes in the midlatitude storm tracks. *J. Atmos. Sci.*, **48**, 2589–2613.

Li, J., and J. X. L. Wang, 2003: A new North Atlantic Oscillation index and its variability. *Adv. Atmos. Sci.*, **20**, 661–676.

Li, S., 2004: Influence of the Northwest Atlantic SST anomaly on the circulation over the Ural Mountains. *J. Meteor. Soc. Japan*, **82**, 971–988.

Li, S., and L. Ji, 2001: Background circulation characteristics of the persistent anomalies of the summertime circulation over the Ural Mountains. *Acta Meteorologica Sinica*, **59**, 280–293. (in Chinese)

Li., S., M. P. Hoerling, S. Peng, and K. M. Weickmann, 2006: The annular response to tropical Pacific SST forcing. *J. Climate*, **19**, 1802–1819.

Li., S., W. A. Robinson, M. P. Hoerling, and K. M. Weickmann, 2007: Dynamics of the extratropical response to a tropical Atlantic SST anomaly. *J. Climate*, **20**,

560–574.

Nitta, T., 1987: Convective activities in the tropical western Pacific and their impacts on the Northern Hemisphere summer circulation. *J. Meteor. Soc. Japan.*, **65**, 165–171.

Ogi, M., Y. Tachibana, and K. Yamazaki, 2003: Impact of the wintertime North Atlantic Oscillation (NAO) on the summertime atmospheric circulation. *Geophys. Res. Lett.*, **30**, 1704, doi: 10.1029/2003GL017280.

Pan, L.-L., 2007: Synoptic eddy feedback and air–sea interaction in the North Atlantic region. *Climate Dyn.*, **29**, 647–659.

Pan, L.-L., F.-F. Jin, and M. Watanabe, 2006: Dynamics of synoptic eddy and low-frequency flow interaction. Part III: Baroclinic model results. *J. Atmos. Sci.*, **63**, 1709–1725.

Peng, S., and J. S. Whitaker, 1999: Mechanisms determining the atmospheric response to midlatitude SST anomalies. *J. Climate*, **12**, 1393–1408.

Peng, S., W. A. Robinson, and S. Li, 2003: Mechanisms for the NAO responses to the North Atlantic SST tripole. *J. Climate*, **16**, 1987–2004.

Ren, H.-L., F.-F. Jin, J.-S. Kug, J.-X. Zhao, and J. Park, 2009: A kinematic mechanism for positive feedback between synoptic eddies and NAO. *Geophys. Res. Lett.*, **36**, L11709, doi: 10.1029/2009GL037294.

Ren, H.-L., F.-F. Jin, and L. Gao, 2012: Anatomy of synoptic Eddy–NAO Interaction through eddy structure decomposition. *J. Atmos. Sci.*, **69**, 2171–2191.

Sardeshmukh, P. D., and B. J. Hoskins, 1988: The generation of global rotational flow by steady idealized tropical divergence. *J. Atmos. Sci.*, **45**, 1288–1251.

Smith, T. M., R. W. Reynolds, T. C. Peterson, and J. Lawrimore, 2008: Improvements to NOAA's historical merged land-ocean surface temperature analysis (1880–2006). *J. Climate*, **21**, 2283–2296.

Sung, M.-K., W.-T. Kwon, H.-J. Baek, K.-O. Boo, G.-H. Lim, and J.-S. Kug, 2006: A possible impact of the North Atlantic Oscillation on the East Asian summer monsoon precipitation. *Geophys. Res. Lett.*, **33**, L21713, doi: 10.1029/2006GL027253.

Takaya, K., and H. Nakamura, 2001: A formulation of a phase-independent wave-activity flux for stationary and migratory quasigeostrophic eddies on a zonally varying basic flow. *J. Atmos. Sci.*, **58**, 608–627.

Trenberth, K. E., G. W. Branstator, D. Karoly, A. Kumar, N.-C. Lau, and C. Ropelewski, 1998: Progress during TOGA in understanding and modeling global teleconnections associated with tropical sea surface temperatures. *J. Geophys. Res.*, **103**, 14291–14324.

Wang, B., and Z. Fan, 1999: Choice of South Asian summer monsoon indices. *Bull. Amer. Meteor. Soc.*, **80**, 629–638.

Watanabe, M., 2004: Asian jet waveguide and a downstream extension of the North Atlantic oscillation. *J. Climate*, **17**, 4674–4691.

Watanabe, M., and M. Kimoto, 2000: Atmosphere–ocean thermal coupling in the North Atlantic: A positive feedback. *Quart. J. Roy. Meteor. Soc.*, **126**, 3343–3369.

Watanabe, M., and F.-F. Jin, 2003: A moist linear baroclinic model: Coupled dynamical–convective response to El Niño. *J. Climate*, **16**, 1121–1139.

Wu, B. Y., and R. H. Zhang, 2011: Interannual variability of the East Asian summer monsoon and its association with the anomalous atmospheric circulation over the mid-high latitudes and external forcing. *Acta Meteorologica Sinica*, **69**, 219–233. (in Chinese)

Wu, R., S. Yang, S. Liu, L. Sun, Y. Lian, and Z. Gao, 2010: Change in the relationship between Northeast China summer temperature and ENSO. *J. Geophys. Res.*, **115**, D21107, doi: 10.1029/2010JD014422.

Wu, R., S. Yang, S. Liu, L. Sun, Y. Lian, and Z. Gao, 2011: Northeast China summer temperature and North Atlantic SST. *J. Geophys. Res.*, **116**, D16116, doi: 10.1029/2011JD015779.

Wu, Z., B. Wang, J. Li, and F.-F. Jin, 2009: An empirical seasonal prediction model of the East Asian summer monsoon using ENSO and NAO. *J. Geophys. Res.*, **114**, D18120, doi: 10.1029/2009JD011733.

Xie, P., and P. A. Arkin, 1997: Global precipitation: A 17-year monthly analysis based on gauge observations, satellite estimates, and numerical model outputs. *Bull. Amer. Meteor. Soc.*, **78**, 2539–2558.

Xie, S.-P., and J. A. Carton, 2004: Tropical Atlantic variability: Patterns, mechanisms, and impacts. *Earth Climate: The Ocean-Atmosphere Interaction*, C. Wang, S.-P. Xie, and J. A. Carton, Eds., Geophysical Monograph, 121–142.

Zhang, Q. Y., and S. Y. Tao, 1998: Influence of Asian mid-high latitude circulation on East Asian summer rainfall. *Acta Meteorologica Sinica*, **56**, 199–211. (in Chinese)

Zhou, T., R. Yu, Y. Gao, and H. Drange, 2006: Ocean-atmosphere coupled model simulation of North Atlantic interannual variability I: Local air-sea interaction. *Acta Meteorologica Sinica*, **64**, 1–17. (in Chinese)

Zuo, J. Q., W. J. Li, H. L. Ren, and L. J. Chen, 2012: Change of the relationship between spring NAO and East Asian summer monsoon and its possible mechanism. *Chinese Journal of Geophysics.*, **55**, 23–34. (in Chinese)